Electronic Supplementary Information

Title:

Effect of CeO_2 support structure on the catalytic performance of ammonia synthesis in an electric field at low temperatures

Authors:

Ryuku Maeda[a], Hiroshi Sampei[a], Reika Nakayama[a], Takuma Higo[a], Yoshiki Koshizuka[a], Yoshiro Bando[b], Tasuku Komanoya[b], Yunosuke Nakahara[b], Yasushi Sekine[a,*]

Affiliations:

*Corresponding author: Yasushi Sekine: ysekine@waseda.jp

[a]Department of Applied Chemistry, Waseda University, 3-4-1, Okubo, Shinjuku, Tokyo 169-8555, Japan

[b]Mitsui Mining and Smelting Co. Ltd., 1333-2, Haraichi, Ageo, Saitama, 362-0021, Japan

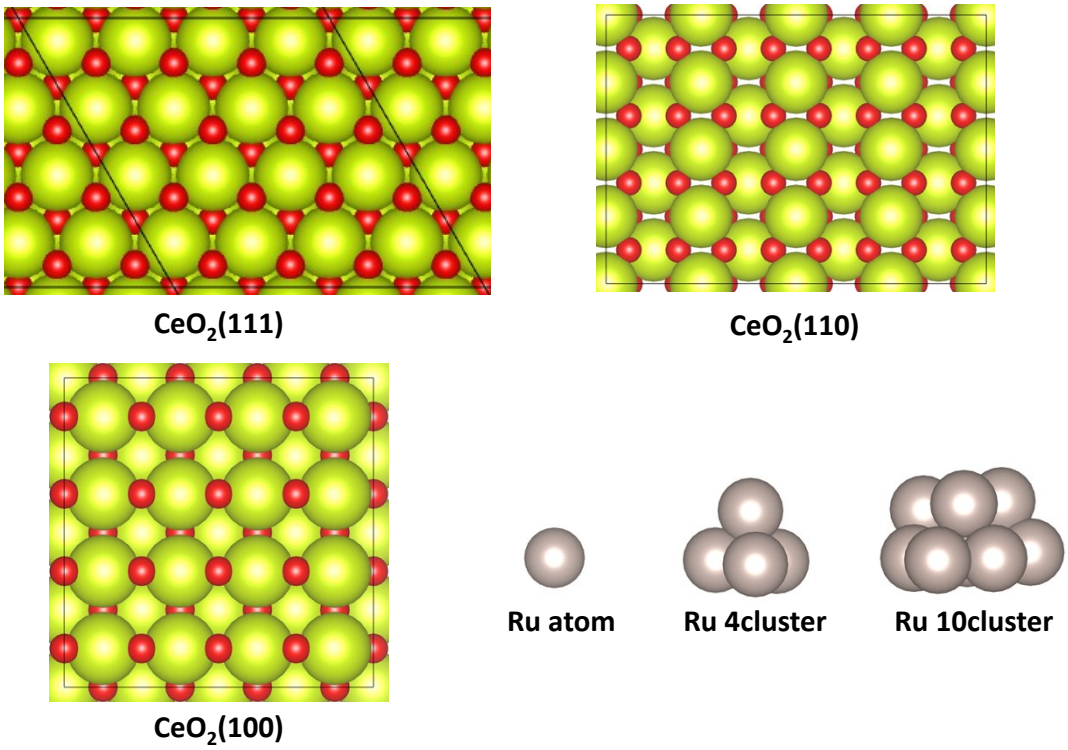

Figure S1 CeO_2 bulk and Ru models for DFT calculations.

It is proposed that the shape of Ru nanoparticles should be as hemispherical as possible. In addition, the particles prefer to expose the most stable surface Ru(0001). Therefore, we prepare the models like hemispheres possessing the top and bottom layers of the (0001) surfaces as the Ru nanoparticle models. The size of the models is limited to up to 10 atoms due to computational costs.

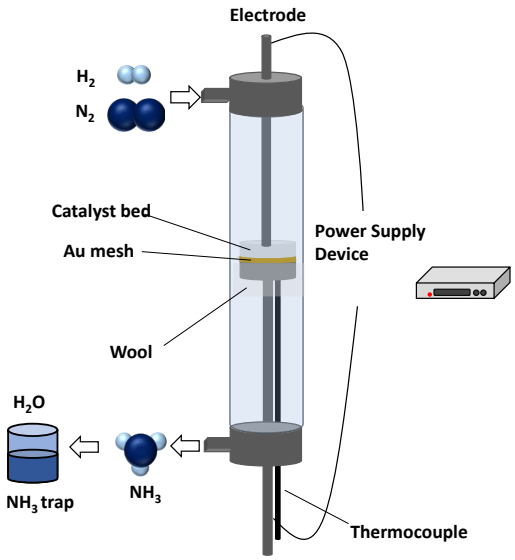

Figure S2 Schematic image of the reactor.

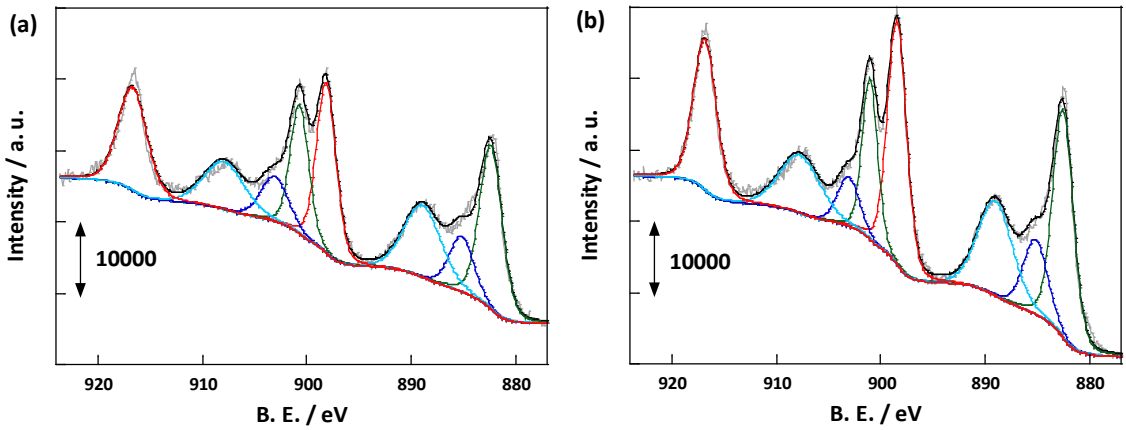

Figure S3 XPS spectrum of Ce 3d after the reaction with the EF

(a)3wt%Ru/CeO_2-p, (b)3wt%Ru/CeO_2-s

Figure S3 shows the Ce *3d* spectra after the reaction with the EF. The ratio of Ce^{3+} after the reaction did not differ significantly between the different catalysts and no change in the electronic state of Ce was observed (Ce^{3+} ratio: 3wt%Ru/CeO_2-p 13.2%, 3wt%Ru/CeO_2-s 12.2%).

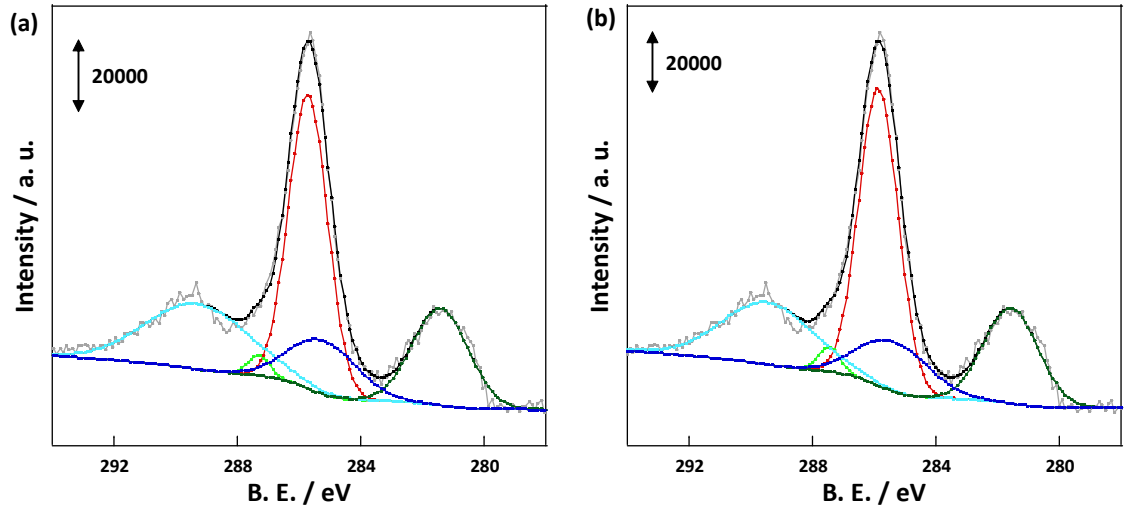

Figure S4 XPS spectrum of C 1*s* after pre-treatment at 673 K;

(a) 3wt%Ru/CeO_2-p, (b) 3wt%Ru/CeO_2-s.

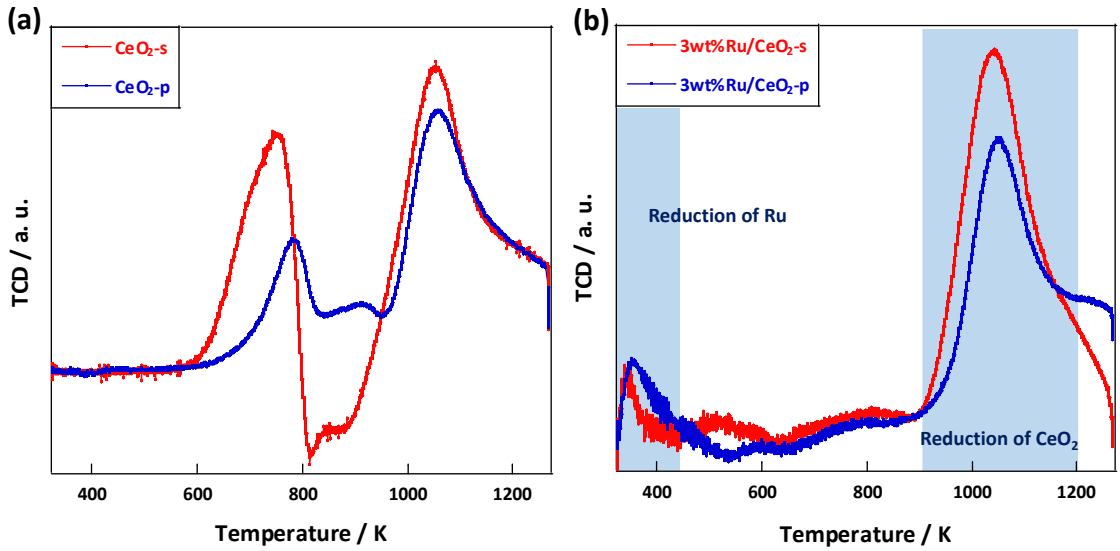

Figure S5 Observation of reduction behaviour by H_2-TPR measurements;
(a) before Ru loading, (b) after Ru loading.

Figure S5 shows the reduction behaviour of each sample in a hydrogen atmosphere. From Figure S5 (a), it is clear that all samples have a reduction peak in the same temperature range. Figure S5 (b) also shows that the reduction peak around 723 K disappears completely after the reduction treatment after Ru loading.

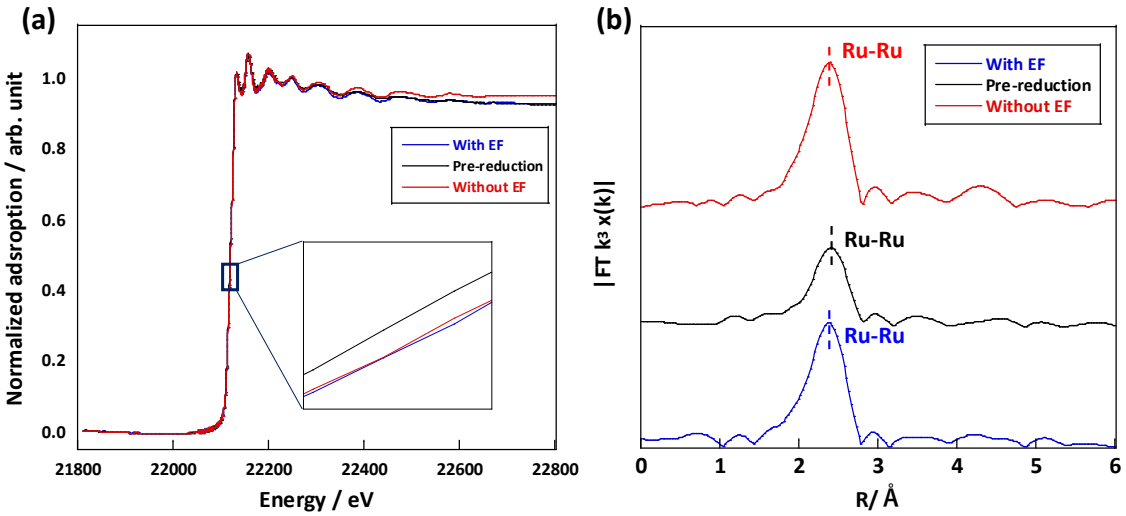

Figure S6 XAFS spectra for each reaction condition of 3wt%Ru/CeO_2-p;
(a) XANES area, (b) FT-EXAFS spectra.

Figure S6 shows a comparison of the *in-situ* XAFS spectra of the Ru *K*-edge when the electric field is applied and not applied. The results show that there is no significant change in the electronic state

of Ru when the reaction conditions are changed, and from Fig. S6(b), no change in physical properties such as bond lengths and coordination numbers is observed.

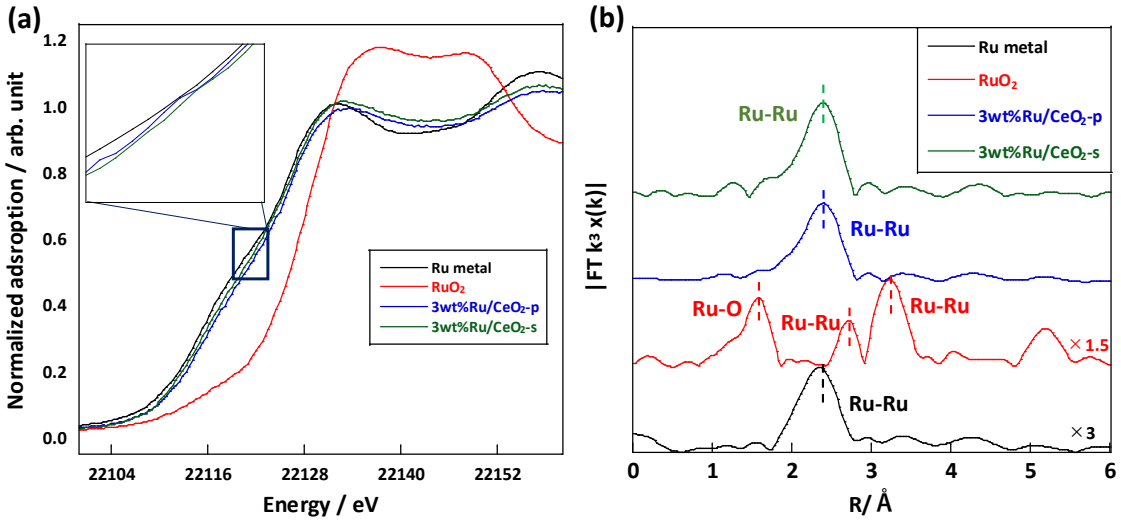

Figure S7 XAFS spectra for each catalyst; (a) XANES area, (b) FT-EXAFS spectra.

Figure S7 shows a comparison of the *in-situ* XAFS spectra of the Ru *K*-edge of each catalyst. The results show that both CeO_2-p and -s show slightly more cationic electronic states than the metal Ru, but can almost be regarded as metal. It is also found that the coordination number and bond lengths do not change significantly between the primary and secondary crystals. These results indicate that the electronic state of Ru does not change with the degree of crystal assembly.

Table S1 Crystallite diameter of each sample from XRD results.

Crystal face	Sample	2θ / degrees	FWHM / °	Crystallite size / Å
Ce(220)	CeO_2-s	47.4	1.55	58.4
	CeO_2-p	47.5	1.32	68.6

Table S2 BET surface area of each catalyst.

Sample	Specific surface area / $m^2\ g^{-1}$
3wt%Ru/CeO_2-s	73.6
3wt%Ru/CeO_2-p	120

Table S3 XPS spectral attribution results for Ce*3d* in 3wt%Ru/CeO_2-p after pre-treatment at 473 K.

Band	Pos	Area	Area%
1	882.3	112997	28.21
2	885.4	34869	8.70
3	888.7	33045	8.25
4	898.2	59510	14.86
5	900.7	75256	18.79
6	903.1	23246	5.80
7	906.9	22008	5.49
8	916.6	39634	9.89

Table S4 XPS spectral attribution results for Ce*3d* in 3wt%Ru/CeO_2-s after pre-treatment at 473 K.

Band	Pos	Area	Area%
1	882.3	111028	27.47
2	885.4	40141	9.93
3	888.7	34330	8.49
4	898.2	57089	14.12
5	900.7	73945	18.30
6	903.1	26761	6.62
7	906.9	22864	5.66
8	916.6	38021	9.41

Table S5 XPS spectral attribution results for Ce*3d* in 3wt%Ru/CeO_2-p after the reaction with the EF.

Band	Pos	Area	Area%
1	882.4	68091	18.87
2	885.2	24925	6.91
3	888.9	49109	13.61
4	898.1	61743	17.11
5	900.7	43908	12.17
6	903.1	22786	6.31
7	907.9	35739	9.90
8	916.7	54585	15.13

Table S6 XPS spectral attribution results for Ce*3d* in 3wt%Ru/CeO_2-s after the reaction with the EF.

Band	Pos	Area	Area%
1	882.6	86857	19.75
2	885.2	33696	7.66
3	889.1	60554	13.77
4	898.5	86112	19.58
5	901.1	45713	10.39
6	903.1	20037	4.56
7	907.8	43489	9.89
8	916.8	63376	14.41